Oxidation of ethanol in the rat brain and effects associated with chronic ethanol exposure

Jie Wang[a,b], Hongying Du[b,c], Lihong Jiang[b], Xiaoxian Ma[b], Robin A. de Graaf[b], Kevin L. Behar[d], and Graeme F. Mason[b,d,1]

[a]State Key Laboratory of Magnetic Resonance and Atomic and Molecular Physics, Wuhan Institute of Physics and Mathematics, Chinese Academy of Science, Wuhan, Hubei 430071, People's Republic of China; [b]Department of Diagnostic Radiology and [d]Department of Psychiatry, School of Medicine, Yale University, New Haven, CT 06511; and [c]College of Food Science and Technology, Huazhong Agricultural University, Wuhan 430070, People's Republic of China

It has been reported that chronic and acute alcohol exposure decreases cerebral glucose metabolism and increases acetate oxidation. However, it remains unknown how much ethanol the living brain can oxidize directly and whether such a process would be affected by alcohol exposure. The questions have implications for reward, oxidative damage, and long-term adaptation to drinking. One group of adult male Sprague–Dawley rats was treated with ethanol vapor and the other given room air. After 3 wk the rats received i.v. [2-^{13}C]ethanol and [1, 2-^{13}C$_2$]acetate for 2 h, and then the brain was fixed, removed, and divided into neocortex and subcortical tissues for measurement of ^{13}C isotopic labeling of glutamate and glutamine by magnetic resonance spectroscopy. Ethanol oxidation was seen to occur both in the cortex and the subcortex. In ethanol-naïve rats, cortical oxidation of ethanol occurred at rates of 0.017 ± 0.002 μmol/min/g in astroglia and 0.014 ± 0.003 μmol/min/g in neurons, and chronic alcohol exposure increased the astroglial ethanol oxidation to 0.028 ± 0.002 μmol/min/g (P = 0.001) with an insignificant effect on neuronal ethanol oxidation. Compared with published rates of overall oxidative metabolism in astroglia and neurons, ethanol provided 12.3 ± 1.4% of cortical astroglial oxidation in ethanol-naïve rats and 20.2 ± 1.5% in ethanol-treated rats. For cortical astroglia and neurons combined, the ethanol oxidation for naïve and treated rats was 3.2 ± 0.3% and 3.8 ± 0.2% of total oxidation, respectively. ^{13}C labeling from subcortical oxidation of ethanol was similar to that seen in cortex but was not affected by chronic ethanol exposure.

13C-NMR catalase | alcohol dehydrogenase | cytochrome P450 | acetaldehyde dehydrogenase

The liver is the major organ for the oxidation of ethanol (Etoh) (1, 2), followed by the stomach and other organs. Acetate (Ac) generated from Etoh by the liver is consumed by the brain (3, 4), where it replaces a significant portion of cerebral glucose metabolism in humans and animals (5–8), either decreasing glucose consumption directly or compensating for glucose consumption decreased by some other effect. However, the brain may also oxidize Etoh (9–14), and that capacity is important with respect to several perspectives. The first step of Etoh oxidation generates acetaldehyde (AA), which is toxic, reactive, and potentially carcinogenic. AA is aversive systemically, as has been observed from the unpleasant effects of disulfuram, an inhibitor of AA dehydrogenase, but it has been shown to be rewarding in parts of the brain (12, 15, 16) especially in the posterior ventral tegmental area (17–19) by activating dopamine neurons (20–22). The liver maintains circulating levels of AA at levels of 20–155 μM (23, 24), and AA has been reported not to penetrate the blood–brain barrier or to penetrate very slowly (23, 25). Thus, if the brain can oxidize Etoh, then intracerebral AA may mediate behavioral, neurochemical, and toxic effects of Etoh in the brain, possibly playing a role in the development of alcohol dependence (6, 16, 26).

AA is difficult to measure in living systems. The concentrations of AA in liver, blood, and brain that occur with drinking lie in the micromolar range (23, 24), in contrast to millimolar levels of Etoh and Ac, and AA rapidly disappears after sample collection due to its volatility. EtOH oxidation and the formation of AA have been measured in brain homogenates (11, 27–30) and cell cultures (31). In a novel approach, Zimatkin and Buben made the measurement in living brain by intraventricular perfusion (9) of anesthetized rats with 180 mM Etoh and measured AA concentrations rising to ~50 μM in the perfusate (23). When the authors perfused the brain with 85–90 mM Etoh, they again observed AA rise in the perfusate with no measurable AA in the blood (9). These studies provide powerful evidence that Etoh oxidation and AA production occur in the living brain. However, cerebral generation of AA is believed to be extremely slow, and Etoh oxidation has not been quantified directly in the awake brain. Neither have the consequences of chronic alcohol exposure on intracerebral oxidation been reported.

It has proven difficult to discriminate by isotopic means the intracerebral oxidation of Etoh from cerebral consumption of Etoh-derived Ac produced in the liver. When hamsters or rats are infused with ^{14}C/^{13}C–Etoh (32), the liver generates ^{14}C/^{13}C–Ac, whose consumption by the brain yields isotopic labeling that is indistinguishable from that of the Etoh. In this study, a combination of [1, 2-^{13}C$_2$]acetate (Ac$_{12}$) and [2-^{13}C]Etoh (Etoh$_2$) provided positional information that differentiated the metabolism of Ac from that of Etoh (Fig. 1). This strategy was used in Etoh-naïve rats and rats exposed to vapor to quantify intracerebral Etoh oxidation and assess the impact of chronic Etoh exposure on intracerebral oxidation of Etoh.

Results

Plasma. Throughout the 2-h infusion, Ac and Etoh were the only substrates whose labeling was detected above natural abundance in the plasma; no labeling appeared for glucose, lactate, and β-hydroxybutyrate. By 30 min after the start of the infusion, blood Etoh$_2$ levels rose to 25.5 ± 0.9 mM and 23.2 ± 1.0 mM (117 and 107 mg/dL) and rose slightly by 2 hr to 28.5 ± 0.9 and 28.1 ± 1.5 mM (131 and 129 mg/dL), respectively, with no differences between the groups (Fig. 2A).

The concentration of Ac increased within 5 min of the start of the coinfusion of Ac$_{12}$ and Etoh$_2$, with the treated animals having more Ac (4.75 ± 0.17 mM) than the naïve group (4.09 ± 0.24 mM) (P = 0.04). The treated group kept a constant level, whereas Ac in the naïve rats decreased to 3.51 ± 0.20 mM at 15 min and stayed constant thereafter (3.66 ± 0.18 mM) (Fig. 2B). The difference in plasma Ac may be associated with metabolic tolerance, an ability of exposed rats to metabolize ethanol more quickly (33, 34), if the rate of acetate clearance is elevated in

www.manaraa.com
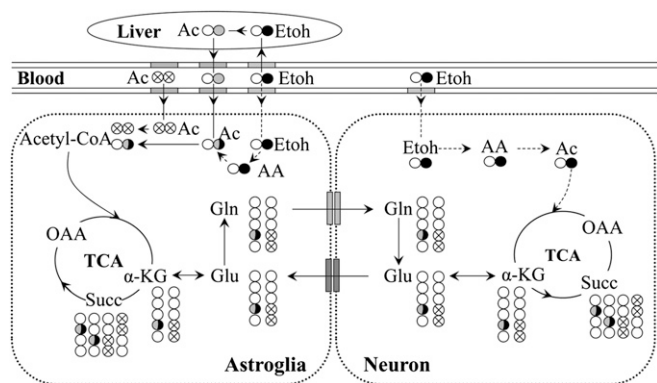
Fig. 1. Model for cerebral metabolism of [1, 2-$^{13}C_2$]Ac and [2-^{13}C]Etoh showing incorporation of ^{13}C into the astroglial and neuronal TCA cycles. The ^{13}C in [2-^{13}C]Etoh is represented by a filled black circle, and the ^{13}C in [2-^{13}C]Ac generated by the liver from [2-^{13}C]Etoh is represented by a filled gray circle. The ^{13}C in [1,2-^{13}C]Ac is represented by two circles marked with an X. The fate of those carbons can be tracked by their colors in their products. Ac inside the astroglia is a mixture of [1,2-^{13}C]Ac transported from the blood (two circles with Xs) and [2-^{13}C]Ac that came from the blood and from intracerebral oxidation of [2-^{13}C]Etoh (half gray/half black). Because neurons import negligible quantities of Ac, the only Ac inside the neuron is from [2-^{13}C]Etoh (filled black circle). The ^{13}C enters the TCA cycle in the neuron, where it arrives in the large neuronal pool of Glu. The Glu is released and taken up by astroglia, where it mixes with the small astroglial pool and is converted to Gln, which flows to the neuron. α-KG, α-ketoglutarate; AA, acetaldehyde; Ac, acetate; Etoh, ethanol; Gln, glutamine; Glu, glutamate; OAA, oxaloacetate; Succ, succinate.

exposed rats, although this study was not designed to address that question.

Fig. 3A shows the ^{13}C spectra from the plasma, with the Ac_{12} doublet around the Ac_2 singlet. The total ^{13}C enrichment of Ac ($Ac_2 + Ac_{12}$) increased to ~85% after 5 min for the Etoh-treated and naïve groups and stayed constant during the infusion (Fig. 2C). To use the steady-state Eq. **1** from *Materials and Methods*, the concentration of Ac and the ratio Ac_2/Ac_{12} had to be maintained constant for the final hour of the procedure, which was achieved here (Fig. 2D). The combination of rapid metabolism of Etoh and the Ac arriving via infusion led to the appearance of ^{13}C-Ac by the first measured plasma time point, 5 min (Fig. 2C). Then the ratio Ac_2/Ac_{12} rose to a stable value after 30 min of infusion (Fig. 2D).

Total Enrichments of Brain Glu_4 and Gln_4. The ^{13}C enrichments of Glu_4 and Gln_4 for cortex and subcortex obtained after 2 hr of infusion are shown in Fig. 4 A and B. Total enrichments of Gln_4 in the Etoh-treated group was significantly higher than the naïve group in both regions ($P = 0.03$ and 0.02 for cortex and subcortex, respectively), demonstrating that after chronic Etoh exposure, the oxidation of Ac and/or Etoh was increased. The total enrichment of Glu_4 in the naïve and treated groups did not differ significantly ($P = 0.4$ and 0.5 for cortex and subcortex, respectively).

Isotopomer Enrichment Patterns of Brain Glu_4 and Gln_4. As a result of spin–spin splitting between the C3 and C4 carbons and the C4 and C5 carbons, it was feasible to differentiate metabolism of Ac_{12}, which labels Gln and Glu always at both C4 and C5, from that of Ac_2, which never labels Gln and Glu at C5. Resonances for Gln_{45} and Glu_{45} were distinguished from those of Gln_4, Glu_4, Gln_{34}, and Glu_{34} (Fig. 3B). The concentrations of Gln_{345} and Glu_{345} were too low to be detected, effectively zero by comparison with the other isotopomers, so only the C_4, C_{34}, and C_{45} labeling were considered for the analysis. The ratio of the Glu_4 singlet resonance (Glu_{4s}) plus the Glu_{34} doublet relative to the Glu_{45} doublet is visibly greater than the ratio of the Ac_2 singlet (Ac_{2s}) to the Ac_{12} doublet, indicating the intracerebral oxidation

of Etoh. Gln also has a singlet and Gln_{34} doublet resonances that are disproportionately large compared with the Gln_{45} doublet, also consistent with Etoh oxidation.

Fig. 4 A and B shows that Gln_{4s} and Gln_{34} were significantly more labeled after chronic Etoh treatment for cortex ($P = 0.02$ and 0.001, respectively) and subcortex ($P = 0.04$ and 0.04, respectively), and the isotopomer analysis allows the source to be ascribed to Ac_2 or $Etoh_2$, as follows.

Quantification of the Intracerebral Etoh Oxidation. Fig. 4 C and D shows the ^{13}C enrichments from Ac_{12}, Ac_2, and $Etoh_2$ in the cortex and subcortex regions, based on the isotopomers observed for Glu_4 and Gln_4. Gln_{Etoh2} was significantly greater ($P = 0.003$) after Etoh chronic treated in cortex, and although Gln_{Ac2} was also higher, the treatment effect did not reach significance ($P = 0.8$). The results indicate significant intracerebral oxidation of Etoh and that the oxidation is increased by chronic exposure to Etoh.

The observed enrichments were used in Eqs. **5** and **6** together with values for rates of the cortical astroglial and neuronal tricarboxylic acid (TCA) cycles and Glu–Gln cycling in the cortex of awake rats (35) (Fig. 5). In astroglia of Etoh-naïve rats, Etoh was oxidized at a rate of 0.017 ± 0.002 μmol/min/g and in neurons 0.014 ± 0.003 μmol/min/g, corresponding to $12.3 \pm 1.4\%$ of astroglial oxidation and $1.7 \pm 0.4\%$ of neuronal oxidation, respectively (Table 1). The cortical Etoh oxidation rate for neurons and astroglia combined, 0.031 ± 0.003 μmol/min/g, corresponds to $3.2 \pm 0.3\%$ of the global brain oxidation of all substrates. Chronic alcohol exposure increased the astroglial Etoh oxidation to 0.028 ± 0.002 μmol/min/g ($P = 0.001$), corresponding to $20.2 \pm 1.5\%$ of astroglial oxidation, with an insignificant effect on neuronal Etoh oxidation ($P = 0.1$). TCA cycle and Glu–Gln cycling rates from three other publications (36–38) were also used with Eqs. **5** and **6** to estimate the rates of cortical Etoh oxidation; in all cases astroglial oxidation of Etoh was found to be elevated significantly (Table S1). In the subcortex, ^{13}C labeling from Etoh oxidation was detected, with no significant impact of Etoh exposure (Fig. 4D). Due to the heterogeneity of the subcortex and its metabolic rates (39), the absolute rates of Etoh oxidation were not estimated. However, the percentages of ^{13}C labeling in the subcortical brain are similar to those in the cortex (Fig. 4 C and D), which suggests that the average Etoh
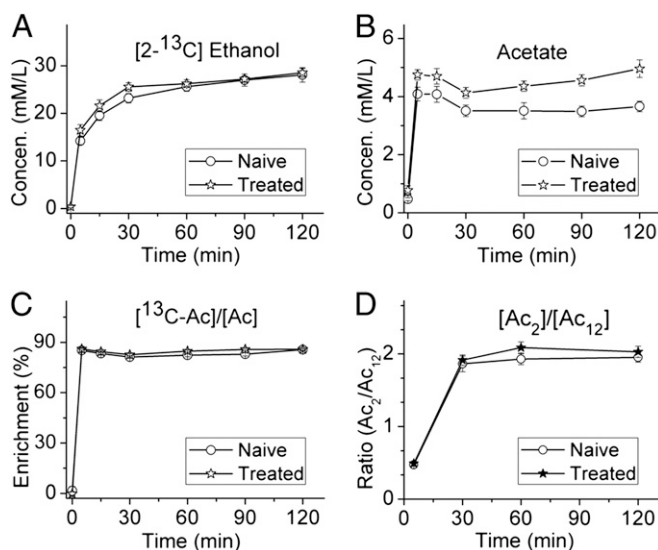

Fig. 2. The concentrations (mM) of ethanol (A) and acetate (B), the total ^{13}C enrichment (%) of acetate (C), and the ratio between [2-^{13}C]acetate (Ac_2) and [1, 2-$^{13}C_2$]acetate (Ac_{12}) in the blood (D), for naïve (10 rats) and ethanol treated (nine rats) groups.
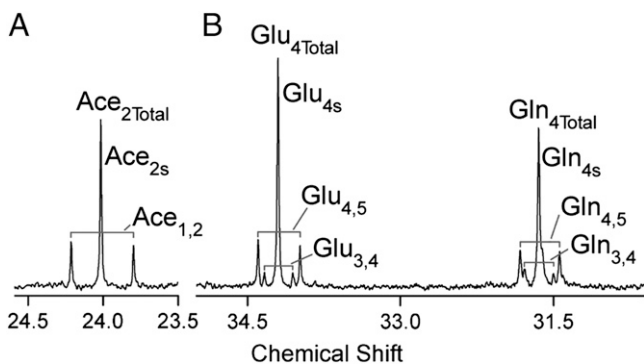
Wang et al.

NEUROSCIENCE

www.manaraa.com

Fig. 3. ^{13}C-NMR spectra of (*A*) plasma and (*B*) brain extracts, showing the disproportionately large singlet/doublet ratios of brain glutamate and glutamine relative to plasma acetate. Ac, acetate; $Ac_{1,2}$, double resonance of $[1,2-^{13}C]$Ac; Ac_{2s}, singlet resonance of $[2-^{13}C]$Ac; Ac_{2Total}, sum of all resonances of Ac labeled at carbon 2; Etoh, ethanol; Gln, glutamine, with analogous notations; Glu, glutamate; $Glu_{3,4}$, doublet resonance of $[3,4-^{13}C]$Glu; Glu_{4s}, singlet resonance of $[4-^{13}C]$Glu; $Glu_{4,5}$, doublet resonance of $[4,5-^{13}C]$Glu; Glu_{4Total}, sum of all resonances of Glu labeled at carbon 4.

oxidation over the subcortical brain comprises a similar fraction of total oxidation.

Discussion

Metabolic Fate of Etoh in the Brain. The first step of Etoh oxidation is its conversion to AA by mitochondrial alcohol dehydrogenase, catalase, or cytochrome P450. Alcohol dehydrogenase has been reported to have very low activity in the brain but appears to be heterogeneously distributed, occurring in some types of neurons (40, 41). Cytochrome P450 also has been shown to metabolize Etoh in the brain in neurons and astroglia, depending on the brain regions (42), but at a rate of 0.00051 μmol/min/g (43), significantly more slowly than the rate of 0.012 μmol/min/g reported for catalase in brain homogenates (calculated from the 3.5–7.1 nmol/mg protein/h (11), using 0.1 g protein/g brain tissue (44)). Furthermore, inhibition of brain catalase activity in mice inhibits many of the pharmacologic effects of ethanol (45), and inhibition or stimulation of catalase activity in brain homogenates, respectively, reduces or increases the formation of AA (14, 15). Thus, evidence suggests that catalase is likely to be a more major contributor to Etoh oxidation in the brain. Inhibition of brain catalase activity in mice inhibits many of the pharmacologic effects of Etoh (45), and inhibition or stimulation of catalase activity, respectively, reduces or increases the formation of AA in brain homogenates (15). Although catalase is found in neurons and astroglia (46, 47), it occurs to a greater extent in neurons (48). From those previous reports of activity in vitro, one can predict a total rate of AA production of ∼0.01 μmol/min/g from alcohol dehydrogenase, catalase, and cytochrome P450 combined, much slower than indicated by the present data in vivo. A possible explanation is the presence of potential cofactors and other environmental conditions that lead to greater activity in vivo than is measured in other preparations. For example, in the presence of glucose oxidase, the activity of catalase for Etoh significantly rises to ∼10-fold (15). In this context, the faster oxidation rates observed in the living rat brain (0.031 and 0.036 μmol/min/g for naïve and treated groups, respectively) are not unreasonable.

The second stage of Etoh metabolism is the conversion of AA to Ac via AA dehydrogenase, which is located in astroglia and neurons in many brain regions (41, 49). The ability of the brain to metabolize aldehydes has long been known (22). It has been shown that the aldehyde-oxidizing capacity of the brain fraction of capillaries and astroglia cells is 5–6 times higher than that of the neurons (49, 50), providing ample capacity to carry out the second step of Etoh oxidation. The rates of oxidation in neurons and glia result from the balance of the latter's higher catalase activity and the slower neuronal aldehyde conversion to Ac.

Ac is considered to be an astroglia-specific substrate, due to a specific Ac-uptake mechanism in astrocytes (51). However, the activity of acetyl-CoA synthetase is greater in neurons than in astrocytes (51). Therefore, a lack of Ac transport into neurons prevents them from oxidizing Ac from the blood, but one would predict that neurons can oxidize Ac that is derived from Etoh intraneuronally.

^{14}C- and ^{11}C- ^{13}C–labeled Etoh have been used to study the fate of Etoh in the brain (10, 52–54). One difficulty has been that isotopically labeled Etoh quickly becomes labeled Ac, whose intracerebral oxidation could not be distinguished from that of Etoh. Xiang and Shen (52) avoided this limitation by using saturation transfer. They detected no exchange between Etoh and AA in the brain, with a detection threshold of 0.001 s^{-1} for the rate constant from Etoh to AA. Given our Etoh levels of ∼28 mM, that saturation transfer detection threshold corresponds to a rate of 1.7 μmol/min/g, which is far greater than our finding of 0.037–0.087 μmol/min/g.

Intracerebral Etoh Oxidation After Chronic Etoh Exposure. It has been shown that the brain consumes Ac and, when Etoh is given to rodents (4–6) and humans (3, 7, 8, 55), decreases its consumption of glucose and increases its use of Ac. Three weeks of Etoh vapor exposure were associated with increased intracerebral Etoh oxidation, at a blood level of ∼28 mM (130 mg/dL). Pharmacokinetic modeling suggested that the change occurred primarily in astroglial Etoh oxidation; the percentage of oxidation supplied by Etoh was higher than in neurons and increased after Etoh exposure.

At least three mechanisms may explain how ethanol oxidation could be increased. (*i*) Chronic Etoh treatment reduces Mg^{2+} in the brain (56, 57). Exposure of brain cells to 10–25 mM EtOH in vitro reduces intracellular Mg^{2+} 15–45% within 10 min in astrocytes and CA1 pyramidal neurons (58). Mg^{2+} deficiency has been associated with increased catalase activity and H_2O_2 production in vitro (59), which might be a potential mechanism for the increase of the oxidation of Etoh in astroglia. (*ii*) Although alcohol dehydrogenase normally has negligible activity in the brain (11), its activity has been reported to increase after chronic Etoh treatment (60). (*iii*) Cytochrome P450 has also been reported to be induced by a moderate dose of 1 g of ethanol in rats weighing 250–300 g (43), with increases of 150–500% in rats treated with 10% ethanol in drinking water for 30 d (61).

Significance of Intracerebral Etoh Oxidation. The current study shows that Etoh can provide energy for the brain, not only from Ac, which was generated in the liver, but also from the directly oxidation in the brain. The small but significant contribution of Etoh to brain oxidation might provide some energetic reward. When Etoh is oxidized directly by the brain, AA is produced within the brain, where it may serve as a pharmacologic reward (62), despite the fact that AA is aversive in the rest of the body. Another likely impact of intracerebral metabolism of Etoh is cumulative damage due to AA toxicity and oxidative damage from free radical generation (63).

Limitations. This study shows that intracerebral oxidation of Etoh occurs and that its rate is increased in astroglia by chronic Etoh treatment. However, the sensitivity of the technique was insufficient to measure oxidation in particular regions of interest, such as the posterior ventral tegmental area (19, 62). A further limitation pertains to the kinetic modeling. The measurements were conducted at an isotopic steady state, which means that the data contain only relative rates: that is, rates of ethanol oxidation relative to the rates of other pathways. Therefore, the absolute rates of ethanol oxidation in glia and neurons, in μmol/min/g, were estimated assuming values for the ratios V_{cycle}/V_{tcaN} and V_{cycle}/V_{tcaA}. A factor to note is that one purpose of this study was to test whether chronic exposure to Etoh could affect intracerebral metabolism of Etoh; it did, but whether such a mechanism is associated with eventual dependence or not is an important question that remains to be investigated.
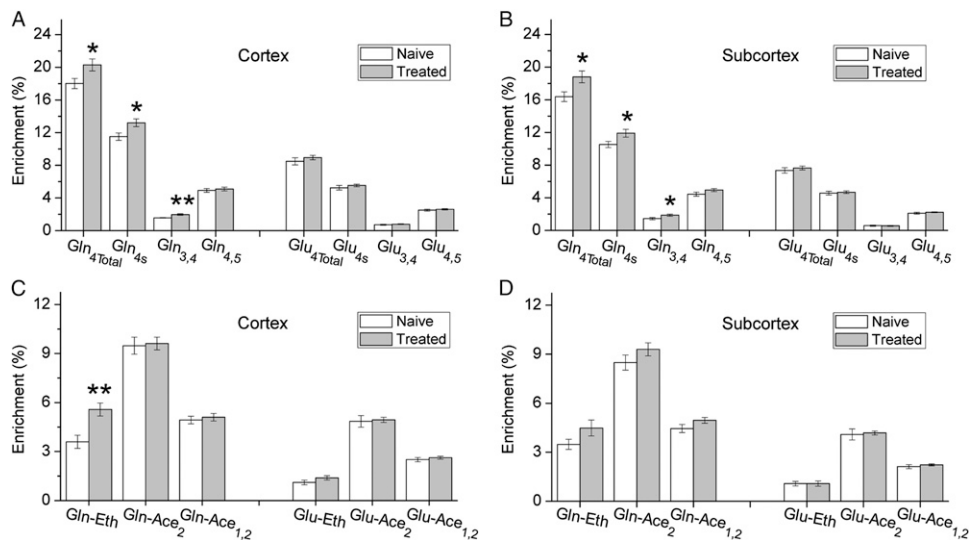
www.manaraa.com

Fig. 4. The ^{13}C labeling in Glu and Gln in the cortex and subcortex for naïve (10 rats) and ethanol-treated (nine rats) groups. (A) The percentage of carbon in cortical Glu and Gln labeled in different patterns: total C4 labeling (Glu and Gln_{4Total}), C4 only (Glu_{4s}, Gln_{4s}), C3,4 (Glu_{34}, Gln_{34}), and C4,5 (Glu_{45}, Gln_{45}). (B) Analogous to A, but for subcortex. (C) The percentage of carbon in Glu and Gln that came from Etoh and Ac. Glu-Ac2, Glu ^{13}C content from [2-^{13}C]Ac; Glu-Ac12, Glu ^{13}C content from [1,2-^{13}C]Ac; Glu-Eth, Glu ^{13}C content from Etoh. The abbreviations for Gln follow the same pattern. (D) Analogous to C but for subcortex. *$P < 0.05$, **$P < 0.01$.

Conclusions

The liver oxidizes most Etoh in the body (1, 2), but there remains some question of how much, if any, Etoh the brain can oxidize directly (9–13). However, the quantification of direct intracerebral Etoh oxidation has been encumbered by hepatic conversion of isotopically labeled Etoh to abundant Ac that circulates in the blood and is readily consumed by the brain. In this experiment, the combination of i.v. infusion of both Ac_{12} and $Etoh_2$ allowed the discrimination of the oxidation of Ac from that of Etoh. The results showed that Etoh can be oxidized by the brain to provide energy, supplying ~12% of astroglial oxidation and ~2% of neuronal oxidation, and that 3 wk of exposure to Etoh vapor was associated with an increase in astroglial Etoh consumption from 12% to 20% of total astroglial oxidation.

Materials and Methods

Strategy for Isotopic Labeling and Estimation of Etoh Oxidation Rates. After the ^{13}C-labeled Ac crosses the blood–brain barrier, it is metabolized exclusively by astroglia (Fig. 1) (51) and labels Glu and Gln (36–38, 51, 64). When Ac_{12} is infused, it enters the brain and yields [4, 5-^{13}C$_2$]Glu and Gln in the first turn of the TCA cycle and [3, 4, 5-^{13}C$_3$]Glu and Gln in the second and subsequent turns (Fig. 1). The total C_{45} and C_{345} labeling is proportional to the percent enrichment (PE) of Ac_{12} in the blood, with a proportionality constant $k_{Ac} = ([4, 5-^{13}C_2]Glu + [3, 4, 5-^{13}C_3]Glu)/Ac_{12}$. When [2-^{13}C]Etoh is infused simultaneously, the liver quickly converts some of it to [2-^{13}C]acetate (Ac_2). In the brain, Ac_2 generates [4-^{13}C] and [3, 4-^{13}C$_2$]Glu and Gln, following the same proportion k_{Ac} observed from the $C_{45}+C_{345}$-glutamate labeled by Ac_{12}. The present study was designed with the intention that $Etoh_2$ would be the only singly labeled substrate in the blood besides Ac_2, so any C_4 and C_{45} labeling of glutamate beyond that expected from the proportion k_{Ac} must come from $Etoh_2$. The ^{13}C-labeling of Gln from $Etoh_2$ was according to:

$$PE_{Gln-Etoh2} = PE_{Gln4+34} - PE_{Gln45+345} * ([Ac_2]/[Ac_{12}]),\quad [1]$$

where PE is the ^{13}C enrichment of Gln at the numbered positions. An equivalent expression exists for Glu.

Etoh oxidation rate was evaluated using steady-state isotopic balance equations:

$$\frac{dGln_4}{dt} = f_{GluA_4} V_{cycle} - f_{Gln_4} V_{cycle} = 0,\quad [2]$$

$$\frac{dGluN_4}{dt} = f_{Gln_4} V_{cycle} + f_{Etoh2} CMRet_N - f_{GluN_4}(V_{cycle} + V_{tcaN}) = 0,\text{ and}\quad [3]$$

$$\frac{dGluA_4}{dt} = f_{GluN_4} V_{cycle} + f_{Ac_2} CMR_{AcA} + f_{Etoh2} CMRet_A - f_{GluA_4}(V_{cycle} + V_{tcaA}) = 0.\quad [4]$$

N and A denote neurons and astroglia; V_{cycle}, V_{tcaA}, and V_{tcaN} are the rates of the glutamate–glutamine neurotransmitter cycle and the astroglial and neuronal TCA cycles, respectively; and $CMRet_N$ and $CMRet_A$ are the cerebral metabolic rates of Etoh in neurons and astroglia. f_{Etoh2} and f_{Ac2} represent the fractional isotopic enrichments of $Etoh_2$ and Ac_2, after subtraction of the 1.1% natural abundance enrichment.

Defining $m_N = V_{cycle}/V_{tcaN}$ and $m_A = V_{cycle}/V_{tcaA}$ yields the following expressions for the rates of neuronal and astroglial Etoh oxidation:

$$CMRet_N = [a - m_N(b-a)]V_{tcaN}\text{ and}\quad [5]$$

$$CMRet_A = [a' - m_A(b'-a')]V_{tcaA},\quad [6]$$

where $a = f_{Glu4s}$, $b = f_{Gln4s}$, $a' = f_{Gln4s} - f_{Gln45} * f_{Ac2/Ac12}$ and $b' = f_{Glu4s} - f_{Glu45} * f_{Ac2/Ac12}$. The values of $CMRet_N$ and $CMRet_A$ can be obtained using published
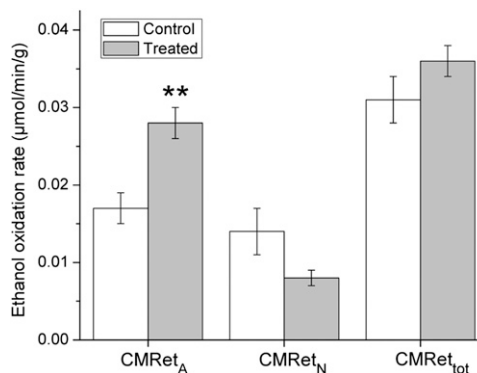

Fig. 5. The cortical oxidation rates of ethanol in astroglia, neurons, and whole brain, calculated using published rates of V_{tcaN}, V_{tcaA}, and V_{cycle}, for naïve (10 rats) and ethanol-treated (nine rats) groups. **$P < 0.01$.

Table 1. The contribution of ethanol to oxidation in neurons, astroglia, and their sum relative to the TCA cycle in awake rats (35)

Cell type	TCA cycle rate, μmol/min/g	Etoh contribution to oxidation		P value
		Naïve	Treated	
Neuron	0.81	1.7 ± 0.4%	1.0 ± 0.1%	0.1
Astroglia	0.14	12.3 ± 1.4%	20.2 ± 1.5%	0.001**
Total	0.95	3.2 ± 0.3%	3.8 ± 0.2%	0.1

**P < 0.01.

rates for V_{cycle}, V_{tcaN}, and V_{tcaA}, and the total oxidation rate of Etoh (CMRet$_{tot}$) is the sum of CMRet$_N$ and CMRet$_A$.

Animal Procedures. All experiments were carried out in accordance with protocols approved by the Yale Animal Care and Use Committee. Nineteen adult male Sprague–Dawley rats (Charles River Labs, Inc.) were maintained on a 12 h/12 h light–dark cycle, and food (Teklad Global 18% Protein Rodent Diet 2018, Harlan Laboratories) and water were available ad libitum. They were allowed a minimum of 2 d to acclimate before the start of the experiments. To familiarize the rats with human interaction and minimize stress on the day of the infusion, they were handled daily until the final day. Room air or Etoh was administered to rats in vapor chambers constructed in-house (65), applying the Etoh vapor 8 h/d for 3 wk. At the start of the exposure period, the naïve rat ($n = 10$) weighed 156.9 ± 1.8g , and the treated rats ($n = 9$) weighed 155.5 ± 1.5 g ($P = 0.572$). The initial vapor level was set at 18~20 mg/L and gradually increased to 23~25 mg/L over the first week. This inhalation model is associated with minimal hepatic dysfunction (66). To monitor the blood Etoh concentration, 200 μL of blood was drawn from the saphenous vein of one rat in each cage each day after 7 h of the day's exposure. With three rats housed per cage, each rat was tested once every 3 d. The blood samples were centrifuged to obtain plasma, and the Etoh concentration measured (Analox GM7, Analox Instruments, Inc.). During the exposure periods, the blood Etoh concentrations reached 150~200 mg/dL, levels that have been shown to induce depressive- and anxiety-like behaviors in rats (67) and slurred speech, double vision, and difficulty walking in humans (68). After 3 wk of Etoh exposure, the weight of the treated rats (301.0 ± 2.8 g) was 3% higher than that of the naïve rats (310.7 ± 2.7 g) ($P = 0.033$).

On the day of infusion, anesthesia was induced with 3% (vol/vol) isoflurane and lowered to 1.5–2.5% for 1–2 min to catheterize one lateral tail vein with a 23-G needle connected with PE-50 tubing (Instech Laboratories, Inc.) (35). The rats then recovered for 30 min, moving and walking freely in the cage before the infusions. Etoh$_2$ (up to 1.373 mg/kg over 2 h) was infused through the tail catheter using a pharmacologically modeled infusion protocol (69). Ac$_{12}$ (up to 322 mg/kg over 2 h) was coadministered by a variable rate infusion over 2 h (2 M dissolved in water, pH = 7.0) according to the following rate schedule: 0–15 s, 1.875 mmol/min/kg; 15 s–4 min, 0.265 mmol/min/kg; 4–14.5 min, 0.15 mmol/min/kg; and 14.5–120 min, 0.075 mmol/min/kg. During the administration, 100 μL blood samples were collected from the saphenous vein at the time points 0, 5, 15, 30, 60, 90, and 120 min; centrifuged at 18,000 × g for 10 min at 2–4 °C; and frozen for later measurement of plasma Etoh$_2$, Ac$_2$, and Ac$_{12}$. After the infusion, the rats were euthanized with focused microwave irradiation (35, 70). The fixed brain was removed and dissected into cortex and subcortex and frozen for later NMR analysis.

Preparation of Plasma Samples for NMR Study. The frozen samples were thawed and centrifuged at 18,000 × g for 5 min. The supernatant was withdrawn and mixed with water to total volume of 150 μL, and an additional 60 μL D$_2$O and 240 μL buffer with 12.5 mM Pi (90 mM K$_2$HPO$_4$ and 35 mM KH$_2$PO$_4$) were added, with 5 mM sodium formate as a concentration and chemical shift reference for ^{1}H-NMR and 150 μL 10 mM [2-^{13}C]glycine as a chemical shift reference for ^{13}C-NMR. The mixture was transferred into a 5 mL NMR tube for NMR analysis.

Preparation of Brain Samples for NMR Study. The frozen brain samples were weighed and placed into a 7 mL homogenizer with 300 μL 0.1 M HCl/mEtoh in a wet ice bath and ground. We added 3 mL ice-cold 60% (vol/vol) Etoh with 150 μL 10 mM [2-^{13}C]glycine as an internal standard, and the mixture was homogenized. The homogenizer was washed with 2 mL ice-cold 60% Etoh, and the total mixture was centrifuged at 18,000 × g for 30 min at 2–4 °C. The supernatant was withdrawn, frozen with liquid nitrogen, and lyophilized for NMR analysis.

The lyophilized extracts were dissolved with 60 μL D$_2$O and 540 μL phosphate buffer. The solution was centrifuged at 18,000 × g for 30 min, and the supernatant was collected for [^{1}H-^{13}C]NMR and ^{13}C-NMR analysis.

NMR Analysis for the Brain Tissue Extracts and Plasma Samples. The measurements were performed at 11.75T on a Bruker vertical bore NMR spectrometer operating at 500.13 MHz for ^{1}H and 125.76 MHz for ^{13}C. ^{1}H-NMR was used to measure the concentrations and total ^{13}C-enrichments of energy substrates in the plasma. ^{1}H-Observed/^{13}C-Edited (POCE) NMR was used to measure the brain concentrations and total ^{13}C-enrichments of Glu and Gln C$_4$ (71). Polarization transfer was used to observe the ^{13}C spectrum to measure plasma Ac$_{12}$ distinctly from Ac$_2$ and to distinguish brain Glu and Gln C$_4$ and C$_{34}$ from Glu and Gln C$_{45}$ and C$_{345}$.

For ^{1}H- and POCE-NMR, the magnetic field homogeneity on each sample was optimized with an automated 3D filed mapping algorithm capable of adjusting up to fifth-order spherical harmonics.

^{1}H-NMR. Spectra were obtained with 12 μs hard-pulse nonselective excitations, with free induction decays acquired as 16,384 complex points. Total concentrations were determined relative to the added formate, and the ^{13}C enrichments of Ac were calculated from the ratio of the areas of the satellite peaks relative to the entire integral of the signal for Ac$_2$.

POCE. Spectra were obtained with the POCE (71), using an 8-ms echo time, 20-s repetition time, 12-ppm sweep width, and 32,768 complex data points. Briefly, the heteronuclear editing method consists of the acquisition of two spin-echo measurements, one with a broadband inversion pulse applied at the ^{13}C frequency and the other without the inversion pulse. The difference between the spectra represents protons bound to ^{13}C (at twice the true intensity), whereas the subspectrum without the inversion pulse represents the protons for ^{13}C-labeled plus the unlabeled compounds (i.e., the total concentrations). The total ^{13}C enrichments of Glu$_4$ and Gln$_4$ were half of the respective ratios between the Glu$_4$ and Gln$_4$ signals in the difference spectrum and subspectrum without the inversion pulse.

^{13}C-NMR. The pulse sequence Insensitive Nuclei Enhanced by Polarization Transfer (INEPT) (72–74) was involved, and 32,768 complex points were acquired after manual adjustment of the magnetic field homogeneity. The enrichments of C$_4$, C$_{34}$, C$_{45}$, and C$_{345}$ of Glu and Gln were calculated according to:

$$f_{Gln4+34} = f_{Gln4Total} * (A_{Gln4} + A_{Gln34})/(A_{Gln4} + A_{Gln34} + A_{Gln45} + A_{Gln345})), \quad [7]$$

where A_{Gln4} is the area of the Gln C$_4$ singlet resonance, A_{Gln34} is the area of the doublet resonance that represents [3, 4-^{13}C$_2$]Gln, and so on for the relevant combinations of labeling. The analogous calculations were performed for $f_{Glu4+34}$ and $f_{Glu45+345}$.

Statistical Analysis. The significance of differences between means of measured parameters in different treatment groups was assessed using two-tailed t tests, assuming unequal variances. All means are presented ± SEM.

1. Lundquist F, Tygstrup N, Winkler K, Mellemgaard K, Munck-Petersen S (1962) Ethanol metabolism and production of free acetate in the human liver. *J Clin Invest* 41(5): 955–961.
2. Norberg A, Jones AW, Hahn RG, Gabrielsson JL (2003) Role of variability in explaining ethanol pharmacokinetics: Research and forensic applications. *Clin Pharmacokinet* 42(1):1–31.
3. Volkow ND, et al. (1990) Acute effects of ethanol on regional brain glucose metabolism and transport. *Psychiatry Res* 35(1):39–48.
4. Roach MK, Reese WN, Jr. (1971) Effect of ethanol on glucose and amino acid metabolism in brain. *Biochem Pharmacol* 20(10):2805–2812.
5. Pawlosky RJ, et al. (2010) Alterations in brain glucose utilization accompanying elevations in blood ethanol and acetate concentrations in the rat. *Alcohol Clin Exp Res* 34(2):375–381.
6. Learn JE, Smith DG, McBride WJ, Lumeng L, Li TK (2003) Ethanol effects on local cerebral glucose utilization in high-alcohol-drinking and low-alcohol-drinking rats. *Alcohol* 29(1):1–9.

www.manaraa.com

7. Volkow ND, et al. (2006) Low doses of alcohol substantially decrease glucose metabolism in the human brain. *Neuroimage* 29(1):295–301.

8. Volkow ND, et al. (2013) Acute alcohol intoxication decreases glucose metabolism but increases acetate uptake in the human brain. *Neuroimage* 64:277–283.

9. Zimatkin SM, Buben AL (2007) Ethanol oxidation in the living brain. *Alcohol Alcohol* 42(6):529–532.

10. Mukherji B, Kashiki Y, Ohyanagi H, Sloviter HA (1975) Metabolism of ethanol and acetaldehyde by the isolated perfused rat brain. *J Neurochem* 24(4):841–843.

11. Zimatkin SM, Liopo AV, Deitrich RA (1998) Distribution and kinetics of ethanol metabolism in rat brain. *Alcohol Clin Exp Res* 22(7):1623–1627.

12. Deng XS, Deitrich RA (2008) Putative role of brain acetaldehyde in ethanol addiction. *Curr Drug Abuse Rev* 1(1):3–8.

13. Towne JC (1964) Effect of ethanol and acetaldehyde on liver and brain monoamine oxidase. *Nature* 201(492):709–710.

14. Zimatkin SM, Deitrich RA (1997) Ethanol metabolism in the brain. *Addict Biol* 2(4): 387–399.

15. Gill K, Menez JF, Lucas D, Deitrich RA (1992) Enzymatic production of acetaldehyde from ethanol in rat brain tissue. *Alcohol Clin Exp Res* 16(5):910–915.

16. Hunt WA (1996) Role of acetaldehyde in the actions of ethanol on the brain—A review. *Alcohol* 13(2):147–151.

17. Rodd-Henricks ZA, et al. (2002) The reinforcing effects of acetaldehyde in the posterior ventral tegmental area of alcohol-preferring rats. *Pharmacol Biochem Behav* 72(1-2):55–64.

18. Deehan GA, Jr., Engleman EA, Ding ZM, McBride WJ, Rodd ZA (2013) Microinjections of acetaldehyde or salsolinol into the posterior ventral tegmental area increase dopamine release in the nucleus accumbens shell. *Alcohol Clin Exp Res* 37(5):722–729.

19. Karahanian E, et al. (2011) Ethanol as a prodrug: Brain metabolism of ethanol mediates its reinforcing effects. *Alcohol Clin Exp Res* 35(4):606–612.

20. Foddai M, Dosia G, Spiga S, Diana M (2004) Acetaldehyde increases dopaminergic neuronal activity in the VTA. *Neuropsychopharmacology* 29(3):530–536.

21. Enrico P, et al. (2009) Acetaldehyde sequestering prevents ethanol-induced stimulation of mesolimbic dopamine transmission. *Drug Alcohol Depend* 100(3):265–271.

22. Erwin VG, Deitrich RA (1966) Brain aldehyde dehydrogenase. Localization, purification, and properties. *J Biol Chem* 241(15):3533–3539.

23. Deitrich R, Zimatkin S, Pronko S (2006) Oxidation of ethanol in the brain and its consequences. *Alcohol Res Health* 29(4):266–273.

24. Kilanmaa K, Virtanen P (1978) Ethanol and acetaldehyde levels in cerebrospinal fluid during ethanol oxidation in the rat. *Neurosci Lett* 10(1-2):181–186.

25. Westcott JY, Weiner H, Shultz J, Myers RD (1980) In vivo acetaldehyde in the brain of the rat treated with ethanol. *Biochem Pharmacol* 29(3):411–417.

26. Quertemont E, et al. (2005) Is ethanol a pro-drug? Acetaldehyde contribution to brain ethanol effects. *Alcohol Clin Exp Res* 29(8):1514–1521.

27. Hamby-Mason R, Chen JJ, Schenker S, Perez A, Henderson GI (1997) Catalase mediates acetaldehyde formation from ethanol in fetal and neonatal rat brain. *Alcohol Clin Exp Res* 21(6):1063–1072.

28. Person RE, Chen H, Fantel AG, Juchau MR (2000) Enzymic catalysis of the accumulation of acetaldehyde from ethanol in human prenatal cephalic tissues: Evaluation of the relative contributions of CYP2E1, alcohol dehydrogenase, and catalase/peroxidases. *Alcohol Clin Exp Res* 24(9):1433–1442.

29. Zimatkin SM, Liopo AV, Slychenkov VS, Deitrich RA (2001) Relationship of brain ethanol metabolism to the hypnotic effect of ethanol. I: Studies in outbred animals. *Alcohol Clin Exp Res* 25(7):976–981.

30. Zimatkin SM, Liopo AV, Satanovskaya VI, Bardina And LR, Deitrich RA (2001) Relationship of brain ethanol metabolism to the hypnotic effect of ethanol. II: Studies in selectively bred rats and mice. *Alcohol Clin Exp Res* 25(7):982–988.

31. Eysseric H, et al. (1997) Characterization of the production of acetaldehyde by astrocytes in culture after ethanol exposure. *Alcohol Clin Exp Res* 21(6):1018–1023.

32. Roach MK, Resse WN, Jr. (1972) (2- 14 C) ethanol as a precursor of glutamine, glutamate, -aminobutyric acid and aspartate in hamster brain in vivo. *Biochem Pharmacol* 21(15):2013–2019.

33. Lumeng L, Li TK (1986) The development of metabolic tolerance in the alcohol-preferring P rats: Comparison of forced and free-choice drinking of ethanol. *Pharmacol Biochem Behav* 25(5):1013–1020.

34. Israel Y, et al. (1979) Studies on metabolic tolerance to alcohol, hepatomegaly and alcoholic liver disease. *Drug Alcohol Depend* 4(1-2):109–118.

35. Wang J, et al. (2010) Regional metabolite levels and turnover in the awake rat brain under the influence of nicotine. *J Neurochem* 113(6):1447–1458.

36. Jiang L, et al. (2009) Recurrent antecedent hypoglycemia alters neuronal oxidative metabolism in vivo. *Diabetes* 58(6):1266–1274.

37. Patel AB, de Graaf RA, Rothman DL, Behar KL, Mason GF (2010) Evaluation of cerebral acetate transport and metabolic rates in the rat brain in vivo using 1H-[13C]-NMR. *J Cereb Blood Flow Metab* 30(6):1200–1213.

38. Shestov AA, Deelchand DK, Ugurbil K, Henry P-G (2011) Elucidating brain metabolism by dynamic 13C isotopomer analysis. *Proc Intl Soc Magn Reson Med Sci Meet Exhib* 19:305.

39. Sokoloff L, et al. (1977) The [14C]deoxyglucose method for the measurement of local cerebral glucose utilization: Theory, procedure, and normal values in the conscious and anesthetized albino rat. *J Neurochem* 28(5):897–916.

40. Kerr JT, Maxwell DS, Crabb DW (1989) Immunocytochemistry of alcohol dehydrogenase in the rat central nervous system. *Alcohol Clin Exp Res* 13(6):730–736.

41. Bühler R, Pestalozzi D, Hess M, Von Wartburg JP (1983) Immunohistochemical localization of alcohol dehydrogenase in human kidney, endocrine organs and brain. *Pharmacol Biochem Behav* 18(Suppl 1):55–59.

42. Hansson T, Tindberg N, Ingelman-Sundberg M, Köhler C (1990) Regional distribution of ethanol-inducible cytochrome P450 IIE1 in the rat central nervous system. *Neuroscience* 34(2):451–463.

43. Warner M, Gustafsson JA (1994) Effect of ethanol on cytochrome P450 in the rat brain. *Proc Natl Acad Sci USA* 91(3):1019–1023.

44. Banayschwartz M, Kenessey A, Deguzman T, Lajtha A, Palkovits M (1992) Protein content of various regions of rat brain and adult and aging human brain. *Age (Omaha)* 15(2):51–54.

45. Escarabajal D, Miquel M, Aragon CMG (2000) A psychopharmacological study of the relationship between brain catalase activity and ethanol-induced locomotor activity in mice. *J Stud Alcohol* 61(4):493–498.

46. Holtzman E, et al. (1973) Notes on synaptic vesicles and related structures, endoplasmic reticulum, lysosomes and peroxisomes in nervous tissue and the adrenal medulla. *J Histochem Cytochem* 21(4):349–385.

47. Holtzman E (1982) Peroxisomes in nervous tissue. *Ann N Y Acad Sci* 386(May): 523–525.

48. Schad A, Fahimi HD, Völkl A, Baumgart E (2003) Expression of catalase mRNA and protein in adult rat brain: Detection by nonradioactive in situ hybridization with signal amplification by catalyzed reporter deposition (ISH-CARD) and immunohistochemistry (IHC)/immunofluorescence (IF). *J Histochem Cytochem* 51(6):751–760.

49. Zimatkin SM, Ostrovskiĭ IuM (1988) [Aldehyde dehydrogenase activity in the barrier brain structures]. *Biull Eksp Biol Med* 106(9):283–284.

50. Tabakoff B, Anderson RA, Ritzmann RF (1977) *Alcohol and Aldehyde Metabolizing Systems*, (Academic, New York), pp 555–565.

51. Waniewski RA, Martin DL (1998) Preferential utilization of acetate by astrocytes is attributable to transport. *J Neurosci* 18(14):5225–5233.

52. Xiang Y, Shen J (2011) In vivo detection of intermediate metabolic products of [1-(13) C]ethanol in the brain using (13) C MRS. *NMR Biomed* 24(9):1054–1062.

53. Mushahwa IK, Koeppe RE (1972) Incorporation of label from [1-14C]ethanol into the glutamate–glutamine pools of rat brain in vivo. *Biochem J* 126(3):467–469.

54. Dimitrakopoulou-Strauss A, et al. (2009) Pharmacokinetic imaging of 11C ethanol with PET in eight patients with hepatocellular carcinomas who were scheduled for treatment with percutaneous ethanol injection. *Radiology* 211(3):681–686.

55. Jiang L, et al. (2013) Increased brain uptake and oxidation of acetate in heavy drinkers. *J Clin Invest* 123(4):1605–1614.

56. Romani AMP (2007) Magnesium homeostasis in mammalian cells. *Front Biosci* 12: 308–331.

57. Altura BM, Weaver C, Gebrewold A, Altura BT, Gupta RK (1998) Continuous osmotic minipump infusion of alcohol into brain decreases brain [Mg2+] and brain bioenergetics and enhances susceptibility to hemorrhagic stroke: An in vivo 31P-NMR study. *Alcohol* 15(2):113–117.

58. Altura BM, Altura BT (1999) Association of alcohol in brain injury, headaches, and stroke with brain-tissue and serum levels of ionized magnesium: A review of recent findings and mechanisms of action. *Alcohol* 19(2):119–130.

59. Yang Y, et al. (2006) Magnesium deficiency enhances hydrogen peroxide production and oxidative damage in chick embryo hepatocyte in vitro. *Biometals* 19(1):71–81.

60. Raskin NH, Sokoloff L (1974) Changes in brain alcohol dehydrogenase activity during chronic ethanol ingestion and withdrawal. *J Neurochem* 22(3):427–434.

61. Anandatheerthavarada HK, et al. (1993) Induction of brain cytochrome P-450IIE1 by chronic ethanol treatment. *Brain Res* 601(1-2):279–285.

62. McBride WJ, et al. (2002) Involvement of acetaldehyde in alcohol addiction. *Alcohol Clin Exp Res* 26(1):114–119.

63. Wu DF, Cederbaum AI (2003) Alcohol, oxidative stress, and free radical damage. *Alcohol Res Health* 27(4):277–284.

64. Oldendorf WH (1973) Carrier-mediated blood-brain barrier transport of short-chain monocarboxylic organic acids. *Am J Physiol* 224(6):1450–1453.

65. Wang J, Jiang LH, Du HY, Mason GF (2012) An ethanol vapor chamber system for small animals. *J Neurosci Methods* 208(1):79–85.

66. Di Luzio NR, Stege TE (1979) Influence of chronic ethanol vapor inhalation on hepatic parenchymal and Kupffer cell function. *Alcohol Clin Exp Res* 3(3):240–247.

67. Getachew B, Hauser SR, Taylor RE, Tizabi Y (2008) Desipramine blocks alcohol-induced anxiety- and depressive-like behaviors in two rat strains. *Pharmacol Biochem Behav* 91(1):97–103.

68. Wallace MJ, Newton PM (2001) *Alcoholism in eLS* (Wiley, New York).

69. Ramchandani VA, O'Connor S (2006) Studying alcohol elimination using the alcohol clamp method. *Alcohol Res Health* 29(4):286–290.

70. Mayne M, Shepel PN, Geiger JD (1999) Recovery of high-integrity mRNA from brains of rats killed by high-energy focused microwave irradiation. *Brain Res Brain Res Protoc* 4(3):295–302.

71. Rothman DL, et al. (1985) 1H-Observe/13C-decouple spectroscopic measurements of lactate and glutamate in the rat brain in vivo. *Proc Natl Acad Sci USA* 82(6): 1633–1637.

72. Burum DP, Ernst RR (1980) Net polarization transfer via a J-ordered state for signal enhancement of low-sensitivity nuclei. *J Magn Reson* 39(1):163–168.

73. Morris GA, Freeman R (1979) Enhancement of nuclear magnetic resonance signals by polarization transfer. *J Am Chem Soc* 101(3):760–762.

74. Morris GA (1980) Sensitivity enhancement in nitrogen-15 NMR: Polarization transfer using the INEPT pulse sequence. *J Am Chem Soc* 102(1):428–429.

NEUROSCIENCE

Wang et al.

www.manaraa.com